

## Sex-related differences in wall remodeling and intraluminal thrombus resolution in a rat saccular aneurysm model

Sandrine Morel, PhD,<sup>1,2</sup> Agnieszka Karol, DVM,<sup>3</sup> Vanessa Graf, MVM,<sup>3</sup> Graziano Pelli,<sup>1</sup> Henning Richter, DVM, PhD,<sup>4</sup> Esther Sutter,<sup>1</sup> Vincent Braunersreuther, PhD,<sup>5</sup> Juhana Frösen, MD, PhD,<sup>6</sup> Philippe Bijlenga, MD, PhD,<sup>2</sup> Brenda R. Kwak, PhD,<sup>1,7</sup> and Katja M. Nuss, DVM<sup>3</sup>

<sup>1</sup>Department of Pathology and Immunology and <sup>7</sup>Department of Medical Specializations—Cardiology, Faculty of Medicine, University of Geneva; <sup>2</sup>Division of Neurosurgery, Department of Clinical Neurosciences, Faculty of Medicine, and <sup>3</sup>Division of Clinical Pathology, Diagnostic Department, Geneva University Hospitals, Geneva; <sup>4</sup>Musculoskeletal Research Unit and <sup>5</sup>Diagnostic Imaging Research Unit, Vetsuisse Faculty, University of Zürich, Switzerland; and <sup>6</sup>Hemorrhagic Brain Pathology Research Group, Department of Neurosurgery, Kuopio University Hospital, Kuopio, Finland

**OBJECTIVE** Intracranial aneurysms (IAs) are more often diagnosed in women. Hormones and vessel geometry, which influences wall shear stress, may affect pathophysiological processes of the arterial wall. Here, the authors investigated sex-related differences in the remodeling of the aneurysm wall and in intraluminal thrombus resolution.

**METHODS** A well-characterized surgical side-wall aneurysm model was used in female, male, and ovariectomized rats. Decellularized grafts were used to model highly degenerated and decellularized IA walls and native grafts to model healthy IA walls. Aneurysm growth and thrombus composition were analyzed at 1, 7, 14, and 28 days. Sex-related differences in vessel wall remodeling were compared with human IA dome samples of men and pre- and postmenopausal women.

**RESULTS** At 28 days, more aneurysm growth was observed in ovariectomized rats than in males or non-ovariectomized female rats. The parent artery size was larger in male rats than in female or ovariectomized rats, as expected. Wall inflammation increased over time in all groups and was most severe in the decellularized female and ovariectomized groups at 28 days compared with the male group. Likewise, in these groups the most elastin fragmentation was seen at 28 days. In female rats, on days 1, 7, and 14, the intraluminal thrombus was mainly composed of red blood cells and fibrin. On days 14 and 28, macrophage and smooth muscle cell invasion inside the thrombus was shown, leading to the removal of red blood cells and deposition of collagen and elastin. On days 14 and 28, similar profiles of thrombus reorganization were observed in male and ovariectomized female rats. However, collagen content in thrombi and vessel wall macrophage content were higher in aneurysms of male rats at 28 days than in those of female rats. On day 28, thrombus coverage by endothelial cells was lower in ovariectomized than in female or male rats. Finally, analysis of human IA domes showed that endothelial cell coverage was lower in men and postmenopausal women than in younger women.

**CONCLUSIONS** Aneurysm growth and intraluminal thrombus resolution show sex-dependent differences. While certain processes (endothelial cell coverage and collagen deposition) point to a strong hormonal dependence, others (wall inflammation and aneurysm growth) seem to be influenced by both hormones and parent artery size.

<https://thejns.org/doi/abs/10.3171/2019.9.JNS191466>

**KEYWORDS** intracranial aneurysm; endothelium; thrombus; sex differences; rat; human; vascular disorders

**ABBREVIATIONS** EC = endothelial cell; IA = intracranial aneurysm; PBS = phosphate-buffered saline; RBC = red blood cell; SMA = smooth muscle actin; SMC = smooth muscle cell; WSS = wall shear stress.

**SUBMITTED** February 22, 2019. **ACCEPTED** September 24, 2019.

**INCLUDE WHEN CITING** Published online December 27, 2019; DOI: 10.3171/2019.9.JNS191466.

**A**NEURYSMAL disease is a degenerative vascular pathology resulting in the deformation of the arterial wall and enlargement of the vessel lumen.<sup>28</sup> Intracranial aneurysms (IAs) are mostly quiescent and asymptomatic but upon rupturing they induce hemorrhagic stroke, potentially leading to severe brain damage and death. The prevalence of IAs is 2%–3% of the adult population, with an average age for detection or rupture close to 50 years.<sup>18,30,40</sup> The incidence of IA rupture is estimated at 9/100,000 inhabitants/year in Western populations, with a female predominance.<sup>1,31,41</sup>

Whereas IAs are more often diagnosed in women than in men,<sup>1,18,31,32,41</sup> there is currently little insight into the underlying factors that contribute to female predominance in IA disease. Two explanations have been proposed: hormonal effects and hemodynamic causes.<sup>20</sup> Studies performed on ovariectomized female rats have supported the idea that estrogens affect the formation<sup>36</sup> and rupture<sup>22,37</sup> of aneurysms, but how they affect the wall remodeling, thrombosis, and neointimal hyperplasia is incompletely understood. Hormones may affect pathophysiological processes in the arterial wall, increasing the likelihood of IA formation. In agreement, limited clinical evidence points to hormone replacement therapy being protective against IA formation.<sup>6,27</sup> The incidence of aneurysmal subarachnoid hemorrhage increases in females after menopause,<sup>35</sup> suggesting that female sex hormones may affect IA wall remodeling and thus the risk of IA rupture. Nevertheless, several studies on a potential association between the use of oral contraception pills and the risk for aneurysmal subarachnoid hemorrhage in premenopausal women have been conducted, but the findings were inconclusive.<sup>19</sup> As the initiation and possibly also the growth and rupture of IAs is known to be driven by wall shear stress (WSS),<sup>10,26</sup> hemodynamic causes have also been proposed as an alternative explanation for the increased IA prevalence in women. Indeed, intracranial blood vessels in women have smaller diameters, which, assuming similar flow conditions in both sexes, would result in higher WSS in females, thus favoring IA formation. There is currently no convincing evidence to support one or the other hypothesis.

In the present study, we investigated in an experimental model of side-wall saccular aneurysms the sex-related differences in the remodeling of the aneurysm wall and intraluminal thrombus resolution. We also investigated whether endothelial cell (EC) coverage in IA domes in humans was associated with patient sex or menopause using the AneuX biobank.<sup>30</sup>

## Methods

Detailed methods are available in the Supplemental Material.

### Rat Aneurysm Protocol

The Helsinki rat model, in which a graft from the thoracic aorta of a donor rat was implanted end-to-side to the infrarenal abdominal aorta of a recipient rat,<sup>24</sup> was used in this study (Fig. 1). A total of 204 10- to 12-week-old Wistar rats were used as experimental animals (females: 55 recipients, 49 donors; males: 26 recipients, 22 donors;

ovariectomized females: 26 recipients, 26 donors). The animals were randomly selected and placed in cages (3 animals per cage) by an animal caretaker who was blinded to the type of treatment. Each cage was allocated to a treatment group. Rats were held in enriched individually ventilated cages with access to standard rat food and water ad libitum. The rats were marked by electronic transponders and tail marks, and the acclimatization phase under test conditions lasted at least 7 days. All animals were monitored and scored twice per day for general well-being. The experiments were performed according to the *Guide for the Care and Use of Laboratory Animals* and to the Swiss national animal protection laws and were approved by the cantonal veterinary authorities.

## Surgical Procedure

### Anesthesia and Perioperative Medication

Anesthesia was induced by isoflurane inhalation in an induction box and maintained via face mask. Additionally, medetomidine (100 µg/kg) and ketamine (20 mg/kg) were injected intraperitoneally, and intraoperative analgesia was achieved by a subcutaneous injection of metamizole (70 mg/kg). During recovery after surgery, 50 µg/kg buprenorphine was given subcutaneously; it was given again after 6–8 hours. The buprenorphine medication was continued for at least 3 days according to pain assessment. During the day, the analgesic agents were given subcutaneously, and overnight the animals received buprenorphine by mouth via drinking water (1 mg glucose and 0.6 mg buprenorphine in 120 ml water).

### Graft Harvesting

Directly before harvesting the graft, the donor animals received an intracardial lethal dosage of potassium chloride. The thoracic cavity was opened, and the thoracic aorta was traced back from the dorsal wall of the thorax upward to the aortic arch. A nonabsorbable 6-0 silk ligature was placed just above the first intercostal artery leaving the aorta. The descending aorta was then cut below the left subclavian artery and then below the ligature. The width and length of the graft were measured.

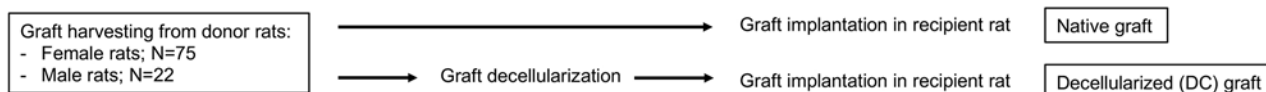
### Graft Decellularization

The untreated graft (native graft) was reimplanted immediately into recipient rats. The saccular aneurysms to be decellularized were first treated as previously reported.<sup>24</sup> Briefly, donor grafts were harvested, and frozen in phosphate-buffered saline (PBS) at –4°C overnight. The next day, the tissue was thawed, rinsed with water, and incubated at 37°C in 0.1% sodium dodecyl sulfate in water for 10 hours. Thereafter, the grafts were washed 3 times and refrozen at –4°C. On the day of implantation, the grafts were thawed at room temperature. Sodium dodecyl sulfate–treated grafts were macroscopically inspected to verify decellularization. Such samples were softer and more fragile than native grafts. Moreover, decellularization was later verified.

### Graft Implantation

After laparotomy, the abdominal aorta was visualized

### A. Graft processing



### B. Timeline procedure

#### D1: Surgery

- Ovariectomy of 26 female rats
- Graft implantation in recipient rat
  - Female rats: N=55
  - Male rats: N=26
  - Ovariectomized rats: N=26



#### D1: Tissue harvesting

- Female-D1: Native graft N=7, DC graft N=7



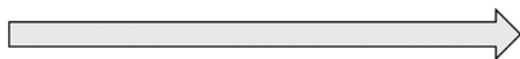
#### D7: MRI and tissue harvesting

- Female-D7: Native graft N=7, DC graft N=6



#### D14: MRI and tissue harvesting

- Female-D14: Native graft N=7, DC graft N=6
- Male-D14: Native graft N=6, DC graft N=6
- Ovariectomized-D14: Native graft N=7, DC graft N=7



#### D28: MRI and tissue harvesting

- Female-D28: Native graft N=6, DC graft N=7
- Male-D28: Native graft N=6, DC graft N=6
- Ovariectomized-D28: Native graft N=6, DC graft N=6

**FIG. 1.** Rat aneurysm protocol. Schematic overview of the graft processing performed on the day of the implantation for the native samples and 2 days before graft implantation for decellularized samples (A) and timeline procedure (B) to study aneurysm growth, wall remodeling, and thrombus organization in defined numbers of female, male, and ovariectomized rats.

and clamped distally to the renal arteries and proximal to the bifurcation. Then, the arteriotomy was performed by cutting out an elliptical part of the ventral vessel wall. Suturing of the end-to-side anastomosis was performed with interrupted sutures. The patency of the aneurysm was confirmed by observing the volume increase of the aneurysm during the peak arterial pulse wave. The small intestines, cecum, and fat mass were then placed back in their correct positions, and the abdominal wall was closed in layers.

#### Ovariectomy

Directly before the graft implantation in the ovariectomized rats, both ovaries were removed after ligation of the ovary vessels.

#### Tissue Harvesting and Macroscopic Measurements

After perfusion of the anesthetized animal with PBS and 4% formalin, the aneurysm was harvested, and its length and width were macroscopically measured. The samples were fixed onto foam strips to avoid curling; the direction of blood flow was indicated. After overnight fixation in 4% formalin, the samples were dehydrated through a series of graded ethanol baths in ascending concentrations and embedded in paraffin.

#### Magnetic Resonance Imaging

All animals underwent MRI postoperatively once a

week after the surgery to determine patency and parent artery (aorta) diameter (Fig. 2A). No aneurysm rupture occurred. The rats were euthanized after 1, 7, 14, or 28 days. After perfusion of the anesthetized animal with PBS and 4% formalin, the aneurysm was harvested, and its length and width were macroscopically measured before overnight fixation in 4% formalin and paraffin. The aneurysm area and parent artery diameter were also measured on histological sections (Fig. 2B).

#### Human IAs

Twenty-six patients diagnosed with unruptured saccular IAs and treated by microsurgery are included in the present study. Patients were recruited at the Geneva University Hospitals. The inclusion criteria in the @neurIST project were 1) IA identified on the basis of angiographic appearance (3D-DSA, 3D-MRA, or 3D-CTA) and availability of surgical documentation; 2) patient age older than 18 years; and 3) informed consent. The study was approved by the ethics committee of the Geneva University Hospitals, Geneva, Switzerland (Geneva Local Ethical Authorization, @neurIST<sup>12</sup>). All procedures were performed in accordance with the Helsinki Declaration of 1975, as revised in 1983. All patients gave consent for their data and biological samples to be used for research in the field of cerebrovascular diseases according to the information and consent forms. After clipping of the aneurysm neck, the resected IA domes were stored as previously described.<sup>30</sup>

## Histological and Immunohistochemical Analyses

Rat and human aneurysms were sectioned at 5  $\mu\text{m}$  and conserved at 4°C as previously described.<sup>30</sup> For histological analysis, rat aneurysm sections were stained routinely with H & E, Martius Scarlet blue (for red blood cells [RBCs] and fibrin), Masson's trichrome (for total collagen), and Victoria blue (for elastin). For immunohistochemical analysis, rat sections were immunolabeled with antibodies recognizing  $\alpha$ -smooth muscle actin ( $\alpha$ -SMA; 1:100, mouse IgG2a antibody, clone 1A4,<sup>33</sup> marker of smooth muscle cells [SMCs]), CD68 (1:500, mouse monoclonal antibody, clone MCA 341R, BioRad, marker of macrophages), or CD31 (1:100, rabbit polyclonal antibody, clone pAK, Dianova, marker of ECs), as previously described.<sup>30</sup> All staining was performed on consecutive sections. Human aneurysm sections were immunolabeled with antibody recognizing CD31, as previously described. Negative controls were performed by incubating sections with PBS instead of the primary antibody. Sections were scanned, and images were processed as previously described.<sup>30</sup> The aneurysm area, intraluminal thrombus area, and positive staining area for  $\alpha$ -SMA, CD68, RBCs, fibrin, collagen, and elastin were quantified using the NIH Image software (NIH AutoExtractor 1.51, National Institutes of Health). Positive staining was expressed as a percentage of the intraluminal thrombus area. For rat aneurysms, the presence of CD68-positive cells inside the aneurysm wall was quantified based on the following scoring system: 0, none (Fig. 3A); 1, few (1–3) spots (Fig. 3B); 2, many (> 4) spots (Fig. 3C); and 3, ubiquitous (Fig. 3D).<sup>25</sup> The number of fragmented elastin fibers in the rat aneurysm walls was counted on sections stained with Victoria blue. For rat aneurysms, coverage of the intraluminal thrombus by ECs (CD31-positive cells and morphology on H & E staining) was quantified using the following scoring system: 0, none; 1, few (1–3) spots; 2, many (> 4) spots; and 3, ubiquitous.<sup>25</sup> For human IAs, EC coverage was calculated as the length of the intraluminal part positively stained for CD31 as a percentage of the total length of the intraluminal portion of the resected dome. All measurements were performed in a blinded manner: surgery, immunostaining, and quantifications were performed by different experimenters, and the allocation of the raw data to each animal was done only after quantifications were finished.

## Statistical Analysis

Comparisons of means were performed using ANOVA and post hoc Tukey's multiple comparison test. Comparisons of medians were performed using the nonparametric Kruskal-Wallis test and post hoc Dunn's multiple comparison test. Comparisons of score distributions were performed using the chi-square test. Differences were considered statistically significant at  $p < 0.05$ .

## Results

### Native or Decellularized Side-Wall Aneurysms Do Not Grow in Female Rats

Native or decellularized grafts were implanted in female rats. Aneurysm growth was investigated on days 1, 7, 14, and 28 postgrafting. Body weights at surgery and death

were not different between the 8 female groups (Supplemental Table 1). Aneurysm patency rates were also similar for all groups. Although some growth of individual aneurysms was observed in the female rat groups on days 7 and 14 (Supplemental Fig. 1A and B), overall no significant difference in aneurysm length, width, or surface area was observed between days 1 and 28 (Supplemental Table 1) or between native and decellularized aneurysms at these time points (Supplemental Table 1). Finally, there was no significant growth within the native and decellularized groups observed over time (Table 1, Supplemental Table 1, and Supplemental Fig. 1A and B).

### Lack of Growth in Aneurysms of Male Rats but Growth of Decellularized Aneurysms in Ovariectomized Female Rats

As the main differences in wall remodeling and thrombus composition occurred in female rats with intact ovaries from day 14 on (see below), experiments with male and ovariectomized female rats included only day 14 and 28 time points. Body weight and graft length and width at surgery were not different between the 4 groups of male rats (Supplemental Table 2) or between the 4 groups of ovariectomized rats (Supplemental Table 3). Aneurysm patency rates were similar for all groups following surgery. In male rats, aneurysm length, width, and surface area did not differ between native and decellularized groups on days 14 and 28 (Table 1, Supplemental Table 2, and Supplemental Fig. 1C and D). Interestingly, an increase in aneurysm length on day 28 was observed in decellularized aneurysms of ovariectomized rats (20%, IQR 12%–31%; Table 1 and Fig. 1E) in comparison with decellularized aneurysms of female rats with intact ovaries (–6%, IQR –13% to 11%; Table 1 and Supplemental Fig. 1A) or male rats (1%, IQR –3% to 6%; Table 1 and Supplemental Fig. 1C).

### Parent Artery Size

On day 28, the body weights were different between female, male, and ovariectomized rats (Supplemental Tables 1–3;  $p < 0.001$ ). Aorta diameters measured in vivo on MRI just before death (Fig. 2A) or ex vivo on histological sections (Fig. 2B) were larger in male rats than in female or ovariectomized rats. No difference in aorta size was observed between native and decellularized groups in female, male, or ovariectomized rats (Fig. 2A and B).

### Sex-Related Differences in Aneurysm Wall Remodeling: Progression of Inflammation and Elastin Fragmentation

Since ovariectomy induced some aneurysm growth in female rats, we investigated possible sex-related differences in inflammation (CD68-positive cells) and wall remodeling (elastin fragmentation). A score defining the level of CD68-positive cells inside the aneurysm wall was given to all samples (representative examples in Fig. 3A–D) using previously described methods.<sup>25</sup> In the female rat group, a few CD68-positive cells were found in the aneurysm wall at baseline after surgery (day 1), but the number of CD68-positive cells considerably increased over time regardless of whether the wall was native or decellularized (Fig. 3E). Infiltration of the aneurysm wall by CD68-positive cells

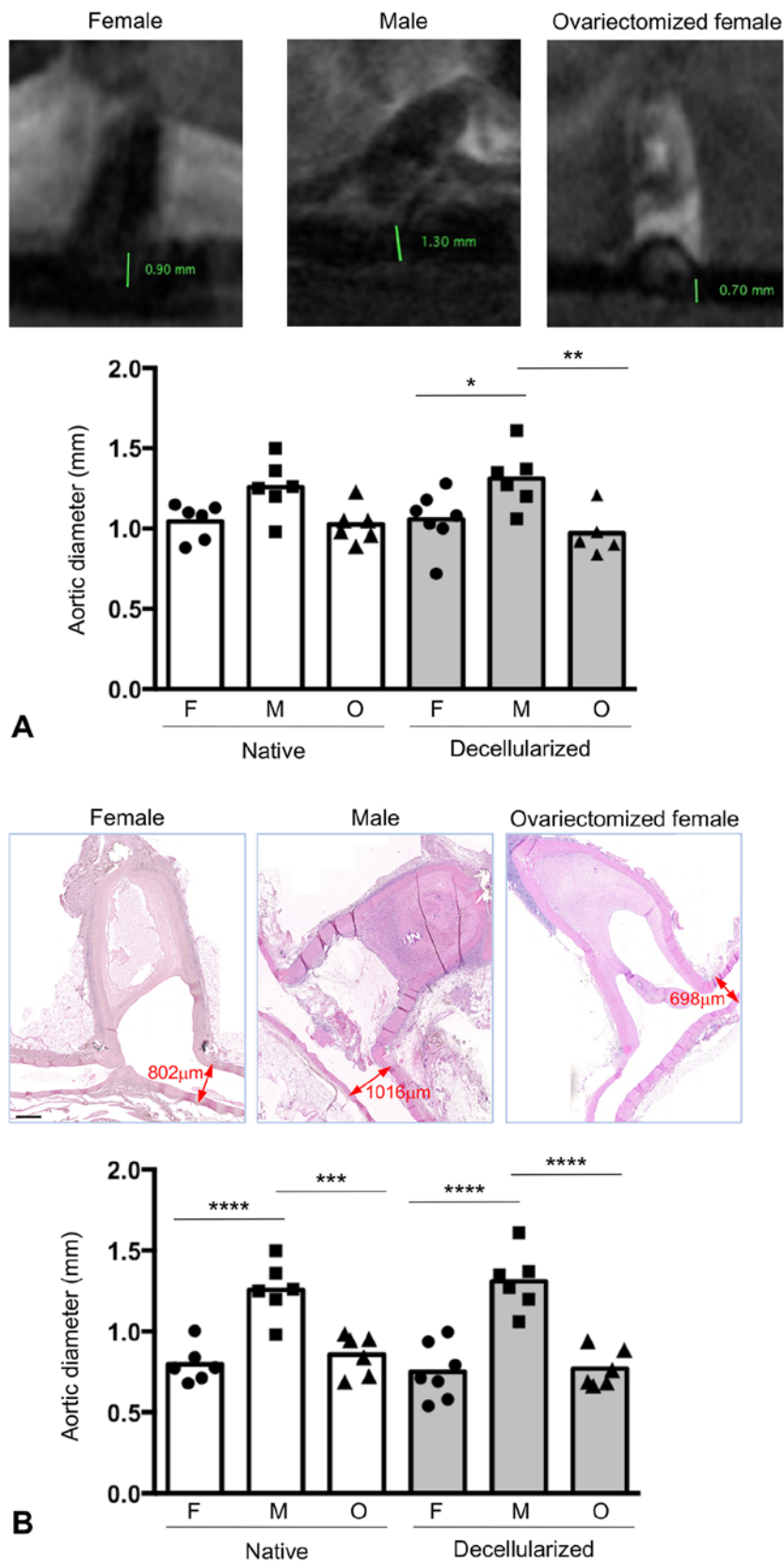


**FIG. 2.** Aorta diameter measured in vivo by MRI just before euthanization on day 28 (A) and ex vivo on histological sections (B) in female (F), male (M), and ovariectomized (O) rats grafted with native and decellularized aneurysms. Bar = 500 μm. Data are shown as individual values and the median. \*\*\*p < 0.001, \*\*\*\*p < 0.0001, nonparametric Mann-Whitney U-test. Figure is available in color online only.

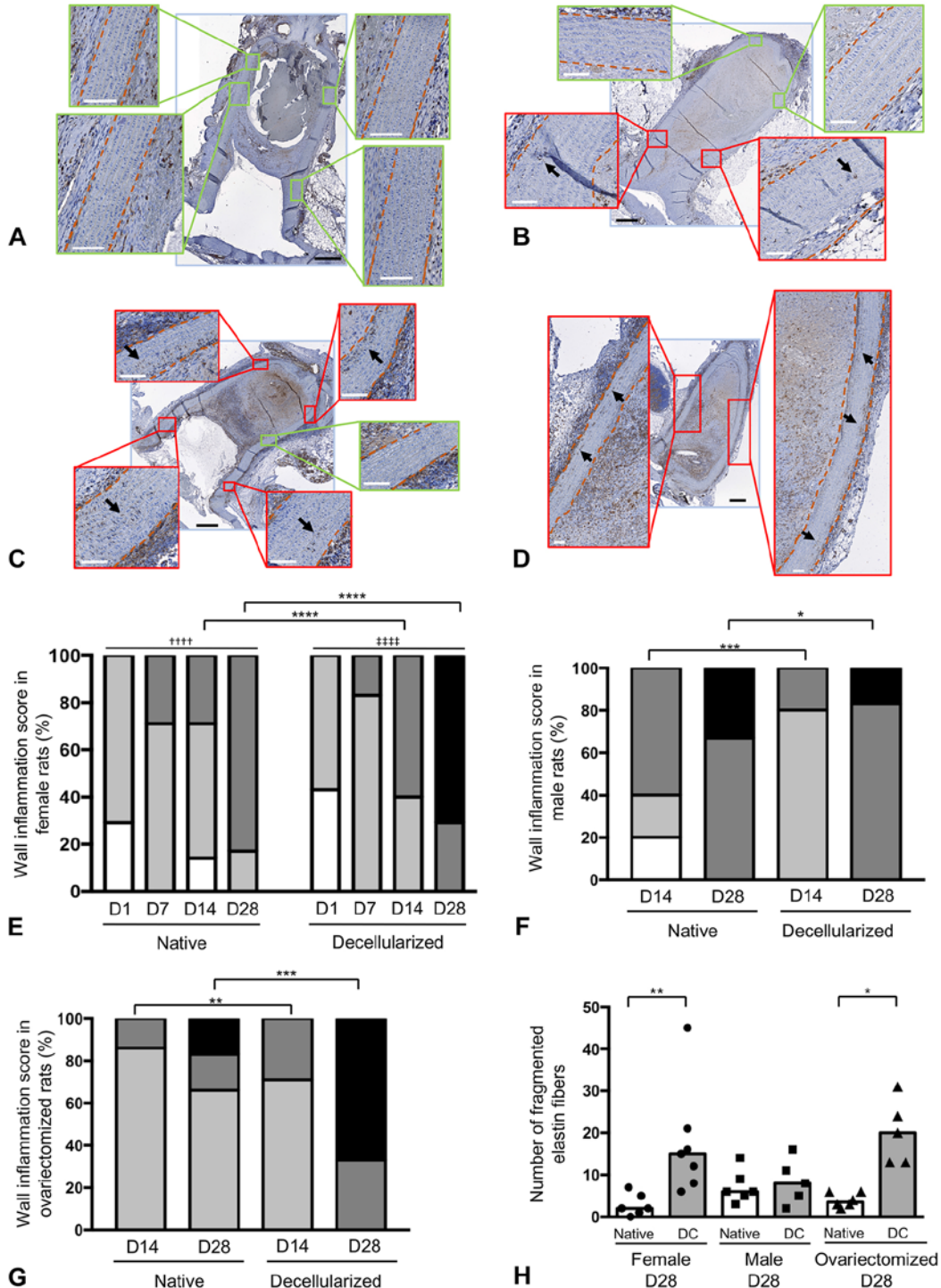


**FIG. 3.** Macrophage infiltration and elastin fragmentation in experimental side-wall aneurysms in female, male, and ovariectomized rats. **A–D:** Representative examples of 4 different levels of macrophage infiltration in the aneurysm media delimited by orange hatched lines. Magnification of regions containing CD68-positive cells is shown in red rectangles and magnification of regions without CD68-positive cells is shown in green rectangles. Some macrophages are indicated by arrows. Black bar = 500  $\mu$ m; white bar = 100  $\mu$ m. **E–G:** Macrophage infiltration in female (E), male (F), and ovariectomized (G) rats was defined by the following scores: 0, none (white bar); 1, few (1–3) spots (light gray bar); 2, many (> 4) spots (dark gray bar); and 3, ubiquitous (black bar). \* $p < 0.05$ , \*\* $p < 0.01$ , \*\*\* $p < 0.001$ , \*\*\*\* $p < 0.0001$ , comparison between native and decellularized aneurysms at the different time points; †††† $p < 0.0001$ , day 28 versus day 1 in native group; ‡‡‡‡ $p < 0.0001$ , day 28 versus day 1 in decellularized group, chi-square test. **H:** Elastin fragmentation in the aneurysm wall of native (white bar) and decellularized (DC; gray bar) grafts in female, male, and ovariectomized rats on day 28. Data are shown as individual values and the median. \* $p < 0.05$ , \*\* $p < 0.01$ , comparison between native and decellularized aneurysms, Kruskal-Wallis test and post hoc Dunn's multiple comparison test. Figure is available in color online only.

**TABLE 1. Side-wall aneurysm growth in female, male, and ovariectomized rats 28 days postgrafting**

	Female		Male		Ovariectomized	
	Native	DC	Native	DC	Native	DC
No. of rats	6	7	6	6	6	6
Median (IQR) aneurysm length change, %	7 (-9 to 14)	-6.0 (-13 to 11)*	11 (8 to 14)	1 (-3 to 6)	20 (14 to 27)	20 (12 to 31)
Median (IQR) aneurysm width change, %	-6 (-13 to 2)	-9 (-30 to 12)	7 (-2 to 25)	-4 (-18 to 5)	-2 (-17 to 21)	-5 (-17 to 28)
Median (IQR) aneurysm area, mm <sup>2</sup>	8 (6 to 11)	8.6 (8.2 to 9.8)	7.9 (7.4 to 8.4)	7 (7 to 10)	8 (5 to 9)	9 (7 to 10)

DC = decellularized.

Changes in aneurysm length and width were calculated as percentages of the aneurysm size at death from aneurysm size at surgery. Aneurysm length and width measured at surgery and death were done macroscopically. The aneurysm area was obtained from H & E-stained sections.

\*  $p < 0.05$ ; comparison of decellularized female and decellularized ovariectomized rats on day 28, Kruskal-Wallis test and Dunn's multiple comparison test.

was significantly higher on days 14 and 28 in decellularized aneurysms than in ones with native walls (Fig. 3E). In contrast, in male rats, the infiltration of CD68-positive cells on days 14 and 28 was lower in decellularized aneurysm walls than in native ones (Fig. 3F). Moreover, the number of CD68-positive cells inside the aneurysm wall increased over time in both groups (Fig. 3F). In ovariectomized rats, infiltration of CD68-positive cells on days 14 and 28 was higher in decellularized than in native aneurysm walls, similar to female rats with intact ovaries (Fig. 3G).

Elastin fragmentation on day 28 associated with infiltration of CD68-positive cells was higher in decellularized aneurysms of both non-ovariectomized and ovariectomized female rats than in the native aneurysm walls in both groups, while no difference between decellularized and native walls was observed in male rats (Fig. 3H). Altogether, these data show that the process of aneurysm wall remodeling is boosted in decellularized grafts (compared with native ones) and display an increasing level of this remodeling in the order of males, females, and ovariectomized animals, suggesting that both small parent artery size and absence of female hormones may enhance the process.

### Sex-Related Differences in Organization of Intraluminal Thrombus

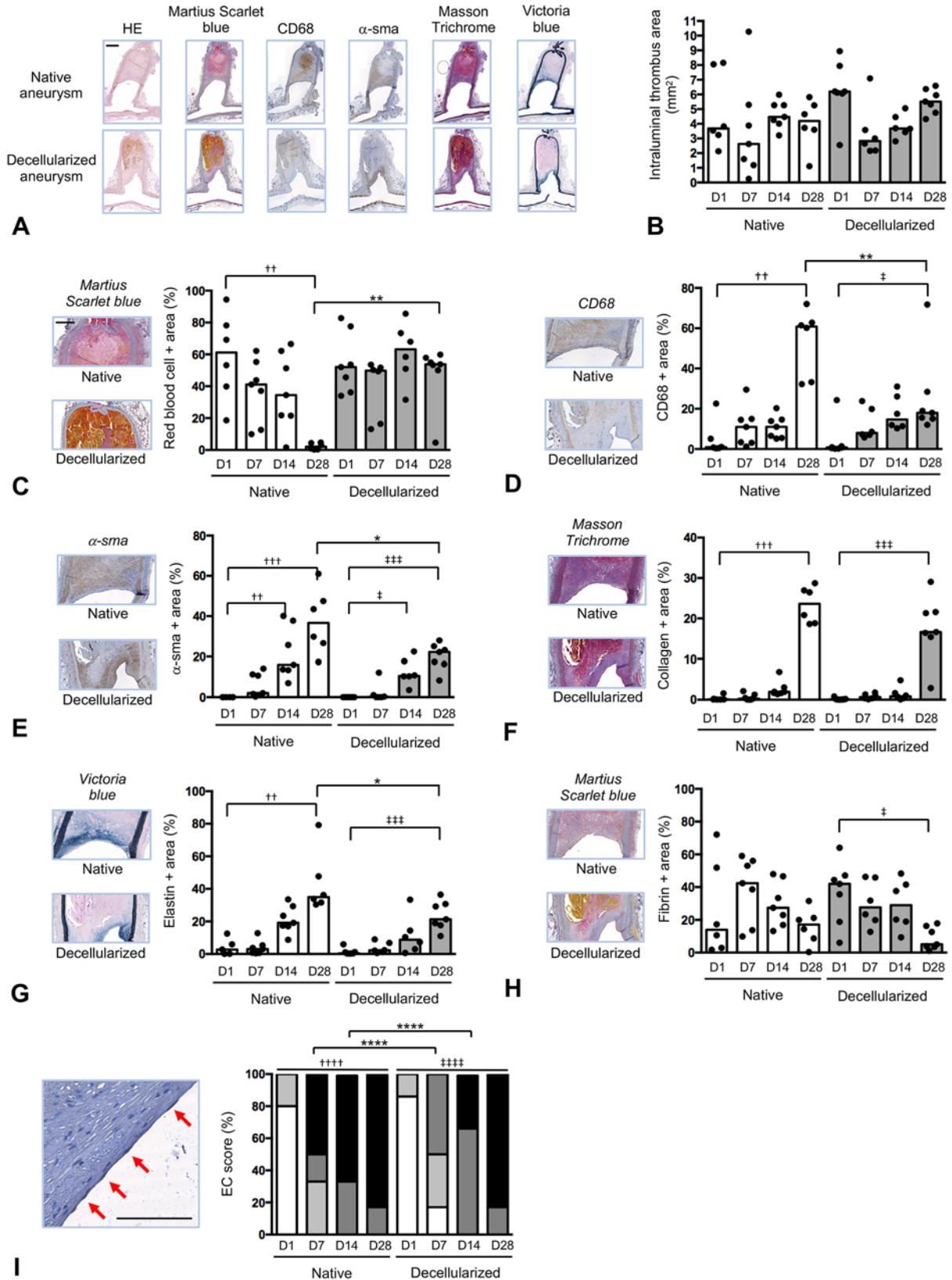
At euthanization, all but 2 aneurysms were partially or totally occluded by thrombi (Supplemental Tables 1–3). Intraluminal thrombus areas, measured on histological sections, were not different between the various time points or between native and decellularized aneurysms in female (Fig. 4A and B) and male (Fig. 5A and B) rats. In ovariectomized rats, the intraluminal thrombus area on day 28 was significantly larger in decellularized aneurysms than in native aneurysms (Fig. 6A and B). Histology showed that in the female rat groups on days 1, 7, and 14, the aneurysm lumen had a layer of thrombus principally composed of RBCs (Fig. 4C) and fibrin (Fig. 4H). At 14 days postsurgery, macrophages (Fig. 4D) and SMCs (Fig. 4E) started to invade the thrombus, leading to the removal of RBCs and deposition of collagen (Fig. 4F) and elastin (Fig. 4G). In decellularized aneurysm grafts, a delayed repair response was observed (Fig. 4, gray bars vs white bars). Thrombus composition in aneurysms of male (Fig. 5C–H) and ovariectomized (Fig. 6C–H) rats showed similar trends to those observed in female aneurysms. Interestingly, the

collagen content of thrombi of aneurysms in the male rats was much higher than that of aneurysms in the female rats (Fig. 5F vs Fig. 4F).

In female rats with intact ovaries, thrombus coverage by ECs was higher in aneurysms with native walls than in those with decellularized walls on days 7 and 14, but not on day 28 (Fig. 4I). In male rats on day 14, EC coverage was lower in decellularized walls than in native walls (Fig. 5I). No difference was observed on day 28. In ovariectomized rats, EC coverage was higher in decellularized walls than in native walls (Fig. 6I), but no difference was observed on day 28. On day 28, EC coverage in native or decellularized aneurysms was significantly lower in ovariectomized rats than in female rats with intact ovaries (score 3, 33%, Fig. 6I vs score 3, 83%, Fig. 4I). In line with the hypothesis that differences in reendothelialization might be related to reduced female sex hormones, male rats had an intermediate EC coverage score between non-ovariectomized and ovariectomized female rats (score 3 in 60% of male decellularized and 67% of native aneurysm walls; Fig. 5I).

### Lower EC Coverage in IAs in Postmenopausal Women

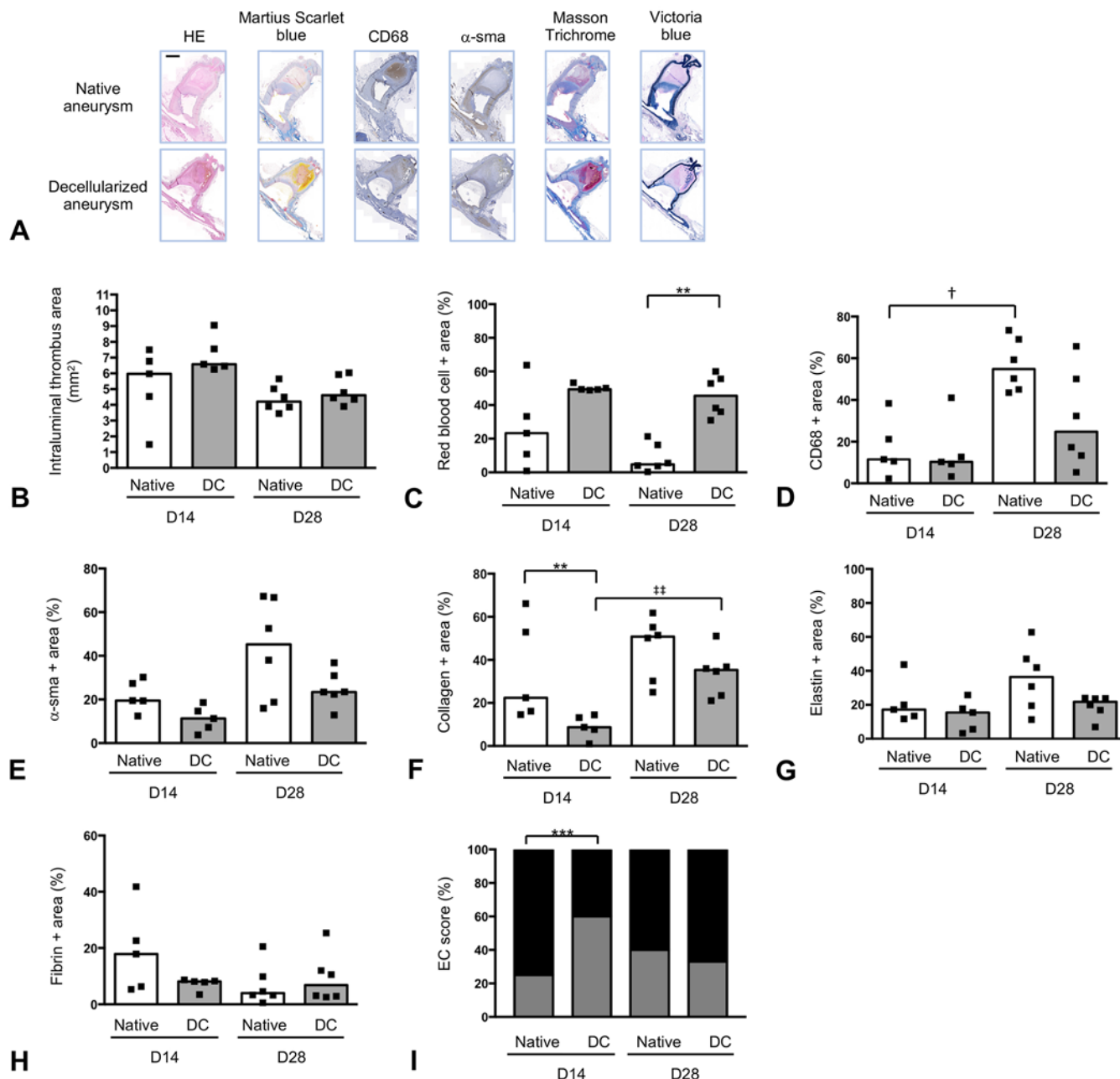
Since our observations from the experimental model suggest that aneurysm growth in ovariectomized rats was not explained by differences in inflammation but rather by impaired reendothelialization of resolving luminal thrombosis, we investigated whether EC coverage of the human IA wall might be affected by sex differences or menopause. IA domes were obtained after clipping in 7 men, 9 women younger than 50 years (younger women), and 10 women older than 50 years (older women; Fig. 7A). The cutoff of 50 years was chosen based on the natural menopausal age in Switzerland.<sup>11</sup> Arterial hypertension, defined as blood pressure greater than 140/90 mm Hg, was present in 43% of men, in 44% of younger women, and in 50% of older women (not significant). IA locations were as follows: middle cerebral artery: 6 men, 6 younger women, and 9 older women; anterior cerebral artery: 1 man, 2 younger women, and 1 older woman; and internal carotid artery: 1 younger woman. The presence of blebs or lobules was exhibited by 5 IAs in men, 6 IAs in younger women, and 4 IAs in older women. An intraluminal thrombus was present in 1 IA in each group. The maximal IA dome diameter (Fig. 7B) and aneurysm neck size (Fig. 7C) were not different between the 3 groups of patients. Intraluminal coverage of IAs by ECs (representative examples in



**FIG. 4.** Intraluminal thrombus composition in female rat aneurysms. **A:** Representative examples of H & E, Martius scarlet blue (RBCs in yellow, fibrin in fuchsia), CD68 (macrophages in brown),  $\alpha$ -SMA (SMCs in brown), Masson's trichrome (collagen in blue), and Victoria blue (elastin in blue) staining performed on native and decellularized aneurysms on day 28. **B:** Intraluminal thrombus area in native (white bar) and decellularized (gray bar) aneurysms from day 1 to day 28 postsurgery. **FIG. 4. (continued)**→



**FIG. 4. C–H:** Intraluminal thrombus composition of native and decellularized aneurysms from day 1 to day 28 characterized for the content of RBCs (C), macrophages (D), SMCs (E), collagen (F), elastin (G), and fibrin (H). Data are shown as individual values and the median. \* $p < 0.05$ , \*\* $p < 0.01$ , native versus decellularized, nonparametric Mann-Whitney U-test; †† $p < 0.01$ , ††† $p < 0.001$ , day 14 or 28 versus day 1, native group; ‡ $p < 0.05$ , ‡‡ $p < 0.001$ , day 14 or 28 versus day 1, decellularized group, nonparametric Kruskal-Wallis test and post hoc Dunn’s multiple comparison test. I: The level of ECs (CD31-positive cells in *brown*, some ECs are indicated by *red arrows*) covering the intraluminal thrombus scored was defined by the following scores: 0, none (*white bar*); 1, few (1–3) spots (*light gray bar*); 2, many (> 4) spots (*dark gray bar*); and 3, ubiquitous (*black bar*). Values are shown in percentages. \*\*\*\* $p < 0.0001$ , native versus decellularized; †††† $p < 0.0001$ , day 28 versus day 1 in native group; ‡‡‡† $p < 0.0001$ , day 28 versus day 1 in decellularized group, chi-square test. Bar = 1 mm (A); 500  $\mu\text{m}$  (C–H); 100  $\mu\text{m}$  (I). Figure is available in color online only.



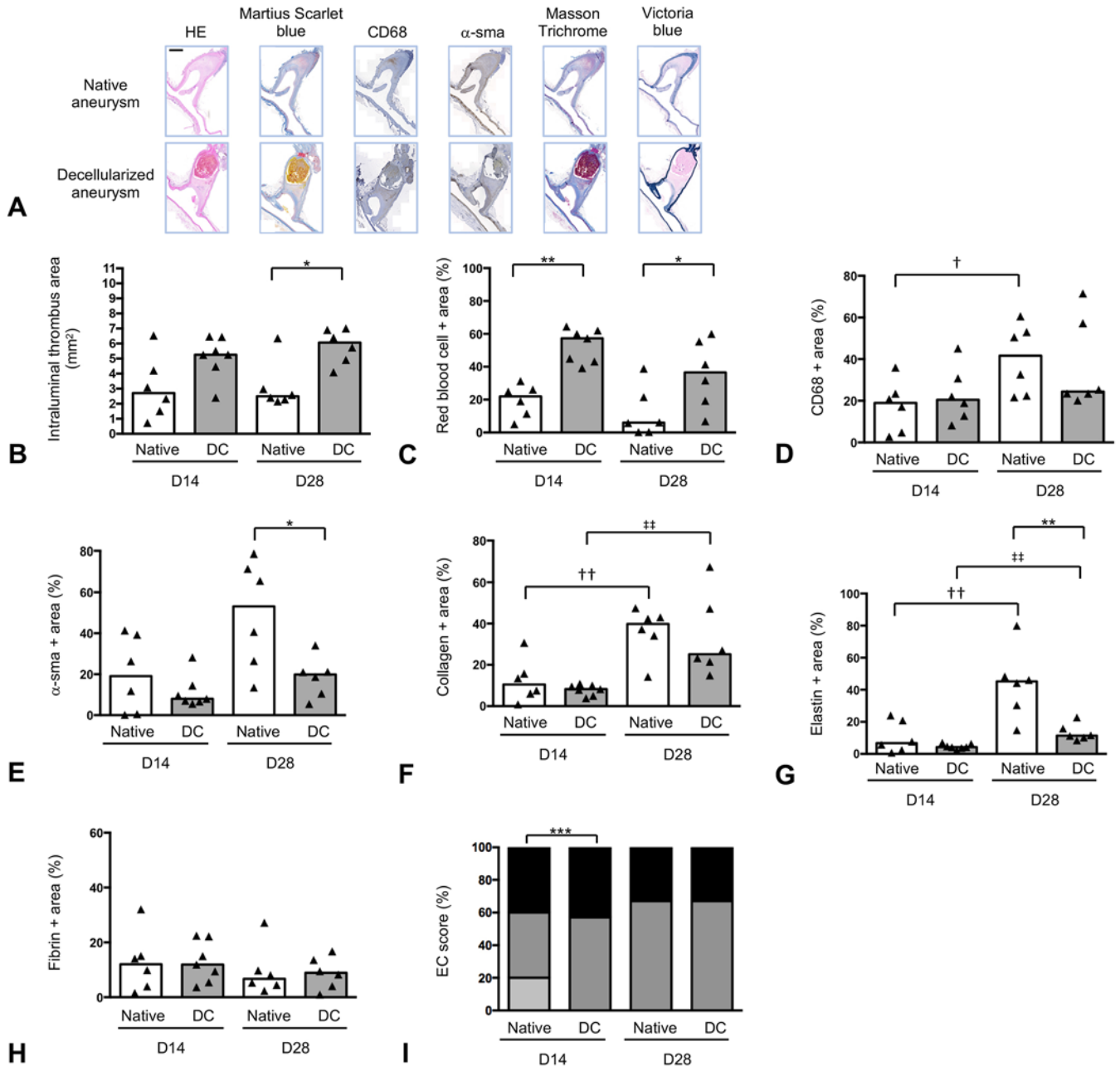
**FIG. 5.** Intraluminal thrombus composition in male rat aneurysms. **A:** Representative examples of H & E, Martius scarlet blue (RBCs in *yellow*, fibrin in *fuchsia*), CD68 (macrophages in *brown*),  $\alpha$ -SMA (SMCs in *brown*), Masson’s trichrome (collagen in *blue*), and Victoria blue (elastin in *blue*) staining performed on native and decellularized aneurysms on day 28. Bar = 1 mm. **B:** Intraluminal thrombus area in native (*white bar*) and decellularized (*gray bar*) aneurysms on days 14 and 28. **C–H:** Intraluminal thrombus composition of native and decellularized aneurysms on days 14 and 28 characterized for the content of RBCs (C), macrophages (D), SMCs (E), collagen (F), elastin (G), and fibrin (H). Data are shown as individual values and medians. \*\* $p < 0.01$ , native versus decellularized; † $p < 0.05$ , day 28 versus day 14, native group; ‡ $p < 0.01$ , day 28 versus day 14, decellularized group, nonparametric Mann-Whitney U-test. **I:** The level of ECs (CD31-positive cells) covering the intraluminal thrombus has been scored as defined in Fig. 4. Values are shown in percentages. \*\*\* $p < 0.001$ , native versus decellularized, chi-square test. Figure is available in color online only.

Fig. 7D) was significantly higher in younger women than in men and older women (Fig. 7E).

### Discussion

Around two-thirds of patients diagnosed with IAs

are women.<sup>1,18,31,32,41</sup> In the present study, we investigated sex-related differences in vessel wall remodeling and intraluminal thrombus resolution using a surgical model of side-wall aneurysms in female, male, and ovariectomized female rats. The saccular nature of this model is well matched to IAs, and the decellularized walls character-



**FIG. 6.** Intraluminal thrombus composition in ovariectomized female rat aneurysms. **A:** Representative examples of H & E, Martius scarlet blue (RBCs in yellow, fibrin in fuchsia), CD68 (macrophages in brown),  $\alpha$ -SMA (SMCs in brown), Masson's trichrome (collagen in blue), and Victoria blue (elastin in blue) staining performed on native and decellularized aneurysms on day 28. Bar = 1 mm. **B:** Intraluminal thrombus area in native (white bar) and DC (gray bar) aneurysms on days 14 and 28. **C–H:** Intraluminal thrombus composition of native and decellularized aneurysms on days 14 and 28 characterized for the content of RBCs (C), macrophages (D), SMCs (E), collagen (F), elastin (G), and fibrin (H). Data are shown as individual values and the median. \* $p < 0.05$ , \*\* $p < 0.01$ , native versus decellularized; † $p < 0.05$ , †† $p < 0.01$ , day 28 versus day 14, native group; ††† $p < 0.01$ , day 28 versus day 14, decellularized group, nonparametric Mann-Whitney U-test. **I:** The level of ECs (CD31-positive cells) covering the intraluminal thrombus has been scored as defined in Fig. 4. Values are shown in percentages. \*\*\* $p < 0.001$ , native versus decellularized, chi-square test. Figure is available in color online only.

ize well the histological features observed in ruptured IAs in humans.<sup>15,24,30</sup> Importantly, this surgical model allows for highly reproducible standardized grafts with minimal variation in aneurysm dimension, location, and relation to the parent artery,<sup>24</sup> resulting in comparable hemodynamic forces within groups.

Thrombus resolution over time proceeds as expected (Figs. 4–6), i.e., a large presence of RBCs and fibrin at the beginning of the process, followed by invasion of macrophages to eliminate these RBCs, thus validating our model. Moreover, SMCs started to invade the thrombus to form a neointima after 2 weeks. On day 28, this process was more important in native aneurysms than in decellularized aneurysms, suggesting that these SMCs originated preferentially from the wall of the graft rather than from the wall of the parent artery or from the circulation. This observation is in accordance with previous studies showing in genetically labeled mice that most intimal cells in a side-wall aneurysm model originate from the aneurysm wall.<sup>14,23</sup> Once inside the thrombus, SMCs produce collagen and elastin, leading to a more mature and stable thrombus. Collagen production inside the thrombus was significantly greater in male than in female rats. In a study of abdominal aortic aneurysms resected from 90 women and men, it was shown that within the thrombus-covered intima-media composite, men had a significantly lower dry weight percentage of elastin and a significantly higher dry weight percentage of collagen when compared with women,<sup>38</sup> suggesting a hormonal effect on extracellular matrix composition. In support of these results, estrogen has been identified as a factor to increase the production of elastin and to reduce collagen deposition in arteries in humans.<sup>9</sup> Our results are in accordance with these previous observations, indicating that such hormonal effects on collagen production are retained among species.

Another major difference between female and male rats observed in our study concerns aneurysm wall inflammation. Indeed, the wall of native aneurysms in male rats had a higher content of macrophages than the aneurysm wall in female or ovariectomized rats (Fig. 3E–G). Estrogens are generally considered to be antiinflammatory, whereas both anti- and proinflammatory properties have been attributed to androgen (reviewed by Gonzales<sup>16</sup>). More particularly, androgens have been described to promote inflammation in the cerebral vasculature, leading to a detrimental outcome following stroke.<sup>7,17</sup> Our results are in agreement with such type of proinflammatory properties of androgens, as we showed a higher macrophage infiltration in the walls of native aneurysms in male rats than in those of female rats. Moreover, wall macrophage content was also higher in native aneurysms of ovariectomized rats than in female rats with intact ovaries, supporting the antiinflammatory properties of estrogens. Furthermore, some clinical and experimental studies have supported the hypothesis that in pathological conditions such as stroke, androgens could have antiinflammatory properties depending on patient age and endogenous levels of the hormone.<sup>8,39</sup> Such data suggest a potential role for androgens in reducing vascular inflammation in the face of a pathological insult.<sup>16</sup> In the decellularized aneurysm walls of male rats, which can be considered as nonphysiological, wall inflammation

was reduced in comparison with native aneurysm walls, sustaining the antiinflammatory properties of androgens in pathological conditions. However, the difference in inflammatory cell infiltration between male and female rats may also be explained by different hemodynamic forces between the two groups. Indeed, associations between WSS and inflammation have been shown in the context of aneurysmal disease.<sup>4</sup> In our study, we showed by *in vivo* and *ex vivo* measurements that the parent artery diameter was larger in male rats than in both groups of female rats (Fig. 2). Such differences in vessel diameter may lead to different WSS patterns between males and females that, in turn, might influence inflammatory cell recruitment to the aneurysm wall.

The presence of estrogen and androgen receptors in SMCs and ECs has been demonstrated in humans and rodents.<sup>16</sup> Androgen excess seems to be associated with endothelial dysfunction in women.<sup>2,34</sup> In our group of ovariectomized rats, the increase in the androgen/estrogen ratio could favor endothelial dysfunction, which might contribute to the highest aneurysm growth observed in this group (Supplemental Table 3). However, disparities in aneurysm growth may also be caused by differences in hemodynamic forces. Indeed, studies using computational fluid dynamics have demonstrated associations between WSS and aneurysm growth. For example, it has been proposed that aneurysm growth due to aneurysm neck enlargement was associated with high WSS and an elevated positive WSS gradient, whereas bleb formation was linked to high focal oscillatory shear index and low WSS.<sup>21</sup> As the parent artery diameter was different between male and female rats (Fig. 2) but the sidewall aneurysms had a similar length and width, hemodynamic forces are expected to be different, which might further contribute to the aneurysm growth observed in ovariectomized rats.

In our human cohort, EC coverage at the intraluminal part of IAs was less in men and in women older than 50 years (mean age  $59 \pm 4$  years and  $62 \pm 2$  years, respectively) than in younger women (mean age  $42 \pm 1$  years). An Italian study showed that endothelial progenitor cells were higher in fertile women (mean age  $41.2 \pm 0.7$  years) than in men, but were not different between postmenopausal women (mean age  $57.2 \pm 1.0$  years) and age-matched men (mean age  $55.7 \pm 0.9$  years).<sup>13</sup> Although the hormone levels of the women involved in this study were not measured to confirm pre- and postmenopausal status, the greater EC coverage measured at the intraluminal surface of IAs in our cohort of women younger than 50 years might thus be due to a larger number of circulating endothelial progenitor cells in this population, which may be a subject of future studies. Another possibility is that EC apoptosis was higher in our population of men and postmenopausal women than in younger women. Indeed, apoptosis has been proposed to contribute to aging phenotypes and/or to the development of certain age-related diseases.<sup>3</sup> Alternatively, it has been shown that the activity of NADPH oxidase, which contributes to oxidative stress and vascular dysfunction, was lower in the cerebral circulation in female rats than in male rats.<sup>29</sup> This negative effect of NADPH oxidase on cell viability and function may contribute to the low presence of ECs in IA domes of men in comparison with women.

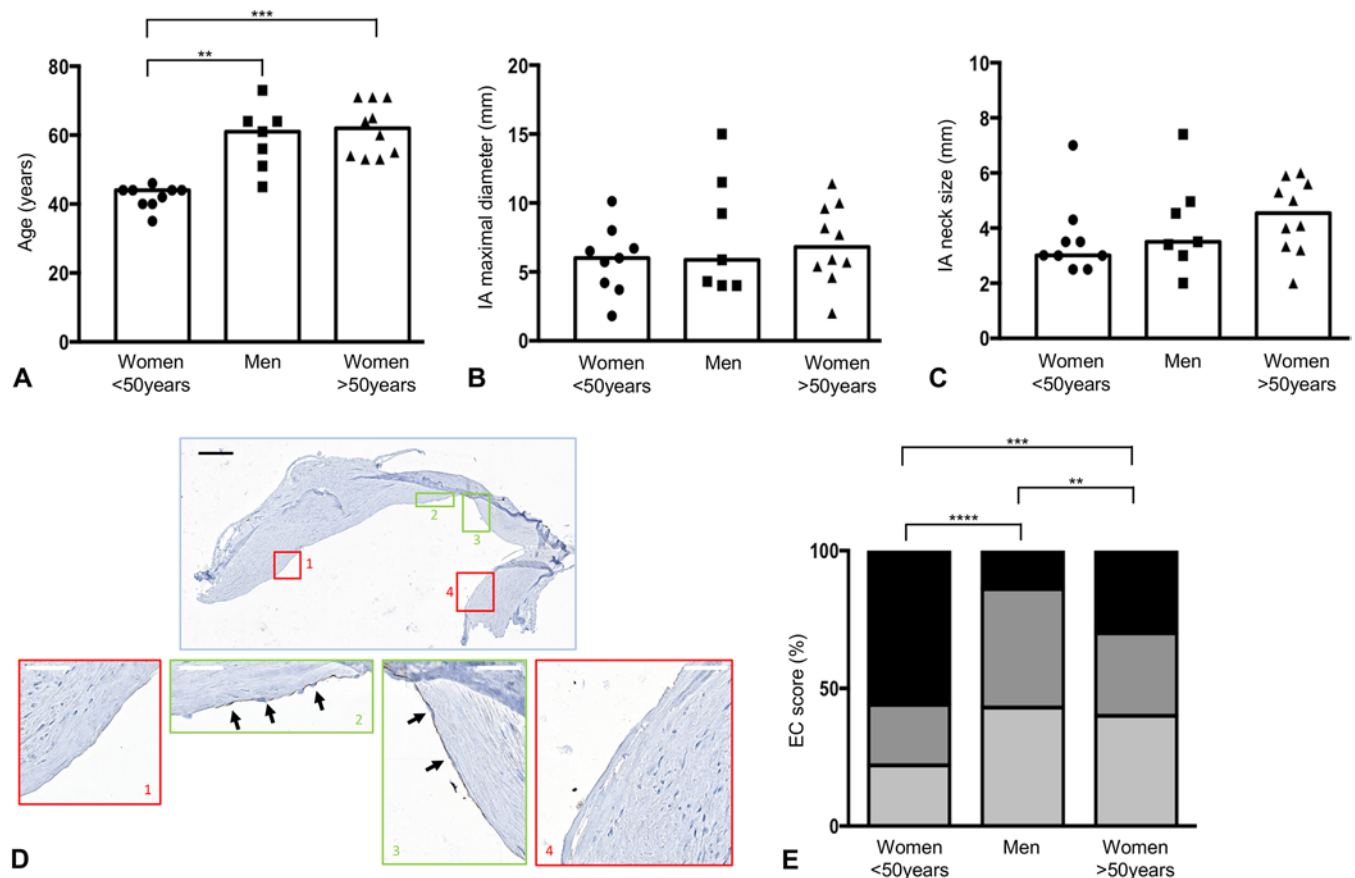


**FIG. 7.** EC coverage in human IAs. **A–C:** Age (A), IA maximal diameter (B), and IA neck size (C) in women younger than 50 years, men, and women older than 50 years. Data are shown as individual values and the median. \*\* $p < 0.01$ , \*\*\* $p < 0.001$ , nonparametric Kruskal-Wallis test and post hoc Dunn's multiple comparison test. **D:** Example of a human IA stained with CD31 antibody showing ECs (brown). Magnification of regions containing CD31-positive cells are shown in green rectangles and magnification of regions without CD31-positive cells are shown in red rectangles. Some ECs are indicated by arrows. Black bar = 200  $\mu\text{m}$ ; white bar = 50  $\mu\text{m}$ . **E:** Intracranial aneurysm EC coverage was defined by the following 3 levels: 1, 0%–25% of the intraluminal part of the resected dome covered by ECs (light gray bar); 2, 25%–50% of the intraluminal part of the resected dome covered by ECs (dark gray bar); and 3, > 50% of the intraluminal part of the resected dome covered by ECs (black bar). \*\* $p < 0.01$ , \*\*\* $p < 0.001$ , \*\*\*\* $p < 0.0001$ , chi-square test. Figure is available in color online only.

When confirmed, the differential presence of ECs at the intraluminal surface of IAs may have implications for clinical strategies chosen for men and (postmenopausal) women. In this respect, a recent study showing that frequent aspirin use decreased the risk of IA rupture more in men than in women, an effect that seems to be mediated by COX-2, is of particular interest.<sup>5</sup>

## Conclusions

Aneurysm growth and intraluminal thrombus resolution show sex-dependent differences. While certain processes, such as EC coverage and collagen deposition, point to a strong hormonal dependence, other processes, such as wall inflammation and aneurysm growth, seem to be influenced by both hormones and parent artery size.

## Acknowledgments

We thank Dr. Marie-Luce Bochaton-Piallat for providing us

with the  $\alpha$ -SMA antibody and for helpful discussions. We thank the medical staff from the Neurosurgery Division of the Geneva University Hospitals for providing us with human intracranial aneurysm domes.

This work was supported by grants from the Swiss SystemsX.ch initiative, evaluated by the Swiss National Science Foundation (to B.R.K., K.M.N., and P.B.), the Foundation Carlos et Elsie De Reuter (to B.R.K. and P.B.), the Swiss Heart Foundation (to B.R.K. and P.B.), and the Novartis Foundation for Medical-Biological Research (to B.R.K.).

## References

1. Bijlenga P, Ebeling C, Jaegersberg M, Summers P, Rogers A, Waterworth A, et al: Risk of rupture of small anterior communicating artery aneurysms is similar to posterior circulation aneurysms. *Stroke* **44**:3018–3026, 2013
2. Calderon-Margalit R, Schwartz SM, Wellons MF, Lewis CE, Daviglius ML, Schreiner PJ, et al: Prospective association of serum androgens and sex hormone-binding globulin with subclinical cardiovascular disease in young adult women: the "Coronary Artery Risk Development in Young Adults"

- women's study. **J Clin Endocrinol Metab** **95**:4424–4431, 2010
3. Campisi J: Cellular senescence and apoptosis: how cellular responses might influence aging phenotypes. **Exp Gerontol** **38**:5–11, 2003
  4. Cebral J, Ollikainen E, Chung BJ, Mut F, Sippola V, Jahromi BR, et al: Flow conditions in the intracranial aneurysm lumen are associated with inflammation and degenerative changes of the aneurysm wall. **AJNR Am J Neuroradiol** **38**:119–126, 2017
  5. Chalouhi N, Starke RM, Correa T, Jabbour PM, Zanaty M, Brown RD Jr, et al: Differential sex response to aspirin in decreasing aneurysm rupture in humans and mice. **Hypertension** **68**:411–417, 2016
  6. Chen M, Ouyang B, Goldstein-Smith L, Feldman L: Oral contraceptive and hormone replacement therapy in women with cerebral aneurysms. **J Neurointerv Surg** **3**:163–166, 2011
  7. Cheng J, Alkayed NJ, Hurn PD: Deleterious effects of dihydrotestosterone on cerebral ischemic injury. **J Cereb Blood Flow Metab** **27**:1553–1562, 2007
  8. Cheng J, Hu W, Toung TJ, Zhang Z, Parker SM, Roselli CE, et al: Age-dependent effects of testosterone in experimental stroke. **J Cereb Blood Flow Metab** **29**:486–494, 2009
  9. Coutinho T: Arterial stiffness and its clinical implications in women. **Can J Cardiol** **30**:756–764, 2014
  10. Diabougua MR, Morel S, Bijlenga P, Kwak BR: Role of hemodynamics in initiation/growth of intracranial aneurysms. **Eur J Clin Invest** **48**:e12992, 2018
  11. Dratva J, Gómez Real F, Schindler C, Ackermann-Liebrich U, Gerbase MW, Probst-Hensch NM, et al: Is age at menopause increasing across Europe? Results on age at menopause and determinants from two population-based studies. **Menopause** **16**:385–394, 2009
  12. Dunlop R, Arbona A, Rajasekaran H, Lo Iacono L, Fingberg J, Summers P, et al: @neurIST – chronic disease management through integration of heterogeneous data and computer-interpretable guideline services. **Stud Health Technol Inform** **138**:173–177, 2008
  13. Fadini GP, de Kreutzenberg S, Albiero M, Coracina A, Pagnin E, Baesso I, et al: Gender differences in endothelial progenitor cells and cardiovascular risk profile: the role of female estrogens. **Arterioscler Thromb Vasc Biol** **28**:997–1004, 2008
  14. Frösen J, Marjamaa J, Myllärniemi M, Abo-Ramadan U, Tulamo R, Niemelä M, et al: Contribution of mural and bone marrow-derived neointimal cells to thrombus organization and wall remodeling in a microsurgical murine saccular aneurysm model. **Neurosurgery** **58**:936–944, 2006
  15. Frösen J, Piippo A, Paetau A, Kangasniemi M, Niemelä M, Hernesniemi J, et al: Remodeling of saccular cerebral artery aneurysm wall is associated with rupture: histological analysis of 24 unruptured and 42 ruptured cases. **Stroke** **35**:2287–2293, 2004
  16. Gonzales RJ: Androgens and the cerebrovasculature: modulation of vascular function during normal and pathophysiological conditions. **Pflugers Arch** **465**:627–642, 2013
  17. Hawk T, Zhang YQ, Rajakumar G, Day AL, Simpkins JW: Testosterone increases and estradiol decreases middle cerebral artery occlusion lesion size in male rats. **Brain Res** **796**:296–298, 1998
  18. Imaizumi Y, Mizutani T, Shimizu K, Sato Y, Taguchi J: Detection rates and sites of unruptured intracranial aneurysms according to sex and age: an analysis of MR angiography-based brain examinations of 4070 healthy Japanese adults. **J Neurosurg** **130**:573–578, 2018
  19. Johnston SC, Colford JM Jr, Gress DR: Oral contraceptives and the risk of subarachnoid hemorrhage: a meta-analysis. **Neurology** **51**:411–418, 1998
  20. Kerkhof PLM, Miller VM (eds): **Sex-Specific Analysis of Cardiovascular Function**. Cham, Switzerland: Springer International Publishing, 2018, Vol 1065
  21. Machi P, Ouared R, Brina O, Bouillot P, Yilmaz H, Vargas MI, et al: Hemodynamics of focal versus global growth of small cerebral aneurysms. **Clin Neuroradiol** **29**:285–293, 2019
  22. Maekawa H, Tada Y, Yagi K, Miyamoto T, Kitazato KT, Korai M, et al: Bazedoxifene, a selective estrogen receptor modulator, reduces cerebral aneurysm rupture in ovariectomized rats. **J Neuroinflammation** **14**:197, 2017
  23. Marbacher S, Frösén J, Marjamaa J, Anisimov A, Honkanen P, von Gunten M, et al: Intraluminal cell transplantation prevents growth and rupture in a model of rupture-prone saccular aneurysms. **Stroke** **45**:3684–3690, 2014
  24. Marbacher S, Marjamaa J, Abdelhameed E, Hernesniemi J, Niemelä M, Frösen J: The Helsinki rat microsurgical sidewall aneurysm model. **J Vis Exp (92)**:e51071, 2014
  25. Marbacher S, Marjamaa J, Bradacova K, von Gunten M, Honkanen P, Abo-Ramadan U, et al: Loss of mural cells leads to wall degeneration, aneurysm growth, and eventual rupture in a rat aneurysm model. **Stroke** **45**:248–254, 2014
  26. Meng H, Tutino VM, Xiang J, Siddiqui A: High WSS or low WSS? Complex interactions of hemodynamics with intracranial aneurysm initiation, growth, and rupture: toward a unifying hypothesis. **AJNR Am J Neuroradiol** **35**:1254–1262, 2014
  27. Mhurchu CN, Anderson C, Jamrozik K, Hankey G, Dunbabin D: Hormonal factors and risk of aneurysmal subarachnoid hemorrhage: an international population-based, case-control study. **Stroke** **32**:606–612, 2001
  28. Michel JB: Biology of vascular wall dilation and rupture, in Krams R, Bäck M (eds): **The ESC Textbook of Vascular Biology**. New York: Oxford University Press, 2017
  29. Miller AA, Drummond GR, Mast AE, Schmidt HH, Sobey CG: Effect of gender on NADPH-oxidase activity, expression, and function in the cerebral circulation: role of estrogen. **Stroke** **38**:2142–2149, 2007
  30. Morel S, Diabougua MR, Dupuy N, Sutter E, Brauersreuther V, Pelli G, et al: Correlating clinical risk factors and histological features in ruptured and unruptured human intracranial aneurysms: the Swiss AneuX Study. **J Neuropathol Exp Neurol** **77**:555–566, 2018
  31. Morita A, Kirino T, Hashi K, Aoki N, Fukuhara S, Hashimoto N, et al: The natural course of unruptured cerebral aneurysms in a Japanese cohort. **N Engl J Med** **366**:2474–2482, 2012
  32. Murayama Y, Takao H, Ishibashi T, Saguchi T, Ebara M, Yuki I, et al: Risk analysis of unruptured intracranial aneurysms: prospective 10-year cohort study. **Stroke** **47**:365–371, 2016
  33. Skalli O, Ropraz P, Trzeciak A, Benzonana G, Gillissen D, Gabbiani G: A monoclonal antibody against alpha-smooth muscle actin: a new probe for smooth muscle differentiation. **J Cell Biol** **103**:2787–2796, 1986
  34. Stanhewicz AE, Wenner MM, Stachenfeld NS: Sex differences in endothelial function important to vascular health and overall cardiovascular disease risk across the lifespan. **Am J Physiol Heart Circ Physiol** **315**:H1569–H1588, 2018
  35. Tabuchi S: Relationship between postmenopausal estrogen deficiency and aneurysmal subarachnoid hemorrhage. **Behav Neurol** **2015**:720141, 2015
  36. Tada Y, Makino H, Furukawa H, Shimada K, Wada K, Liang EI, et al: Roles of estrogen in the formation of intracranial aneurysms in ovariectomized female mice. **Neurosurgery** **75**:690–695, 2014
  37. Tada Y, Wada K, Shimada K, Makino H, Liang EI, Murakami S, et al: Estrogen protects against intracranial aneurysm rupture in ovariectomized mice. **Hypertension** **63**:1339–1344, 2014

38. Tong J, Schriefel AJ, Cohnert T, Holzapfel GA: Gender differences in biomechanical properties, thrombus age, mass fraction and clinical factors of abdominal aortic aneurysms. **Eur J Vasc Endovasc Surg** **45**:364–372, 2013
39. Uchida M, Palmateer JM, Herson PS, DeVries AC, Cheng J, Hurn PD: Dose-dependent effects of androgens on outcome after focal cerebral ischemia in adult male mice. **J Cereb Blood Flow Metab** **29**:1454–1462, 2009
40. Vlak MH, Algra A, Brandenburg R, Rinkel GJ: Prevalence of unruptured intracranial aneurysms, with emphasis on sex, age, comorbidity, country, and time period: a systematic review and meta-analysis. **Lancet Neurol** **10**:626–636, 2011
41. Wiebers DO, Whisnant JP, Huston J III, Meissner I, Brown RD Jr, Piepgras DG, et al: Unruptured intracranial aneurysms: natural history, clinical outcome, and risks of surgical and endovascular treatment. **Lancet** **362**:103–110, 2003

---

## Disclosures

The authors report no conflict of interest concerning the materials or methods used in this study or the findings specified in this paper.

## Author Contributions

Conception and design: Frösen, Bijlenga, Kwak, Nuss. Acquisition of data: Morel, Karol, Graf, Pelli, Richter, Sutter, Braunersreuther, Nuss. Analysis and interpretation of data: Morel, Karol, Graf, Richter. Drafting the article: Morel, Frösen, Bijlenga, Kwak. Criti-

cally revising the article: Morel, Karol, Graf, Frösen, Bijlenga, Kwak, Nuss. Reviewed submitted version of manuscript: all authors. Approved the final version of the manuscript on behalf of all authors: Morel. Statistical analysis: Morel. Administrative/technical/material support: Morel, Pelli, Sutter, Braunersreuther. Study supervision: Bijlenga, Kwak, Nuss.

## Supplemental Information

### Online-Only Content

Supplemental material is available with the online version of the article.

*Supplemental Material.* <https://thejns.org/doi/suppl/10.3171/2019.9.JNS191466>.

### Previous Presentations

A portion of this work was presented at the 9th Center for Applied Biotechnology and Molecular Medicine Symposium, Zurich, Switzerland, November 8, 2018.

## Correspondence

Sandrine Morel: University of Geneva, Switzerland. sandrine.morel@unige.ch.